Biochimica et Biophysica Acta 1828 (2013) 1415–1423

Contents lists available at SciVerse ScienceDirect

Biochimica et Biophysica Acta

journal homepage: www.elsevier.com/locate/bbamem

Grazing Incidence X-ray Diffraction and Brewster Angle Microscopy studies on domain formation in phosphatidylethanolamine/cholesterol monolayers imitating the inner layer of human erythrocyte membrane

Paweł Wydro *, Michał Flasiński, Marcin Broniatowski

Faculty of Chemistry, Jagiellonian University, Ingardena 3, 30-060 Kraków, Poland

ARTICLE INFO

Article history:
Received 4 November 2012
Received in revised form 21 January 2013
Accepted 30 January 2013
Available online 8 February 2013

Keywords:
Phosphatidylethanolamine
Cholesterol
Model cytosolic layer
Domain formation

ABSTRACT

In this work the properties of monomolecular films composed of 1-stearoyl-2-oleoyl-*sn*-glycero-3-phosphoethanolamine (SOPE) and cholesterol, differing in lipid proportion, were investigated in the context of domain formation in the inner leaflet of membrane. To perform comprehensive analysis of the studied model systems the Langmuir monolayer experiments were performed in combination with Brewster angle microscopy (BAM) and Grazing Incidence X-ray Diffraction (GIXD) techniques. The analysis of the collected data proved non-ideal behavior of the investigated films. It was found that cholesterol at its lower concentration in the system (10%) is of disturbing influence on SOPE film. Further addition of cholesterol into phospholipids film (33, 50, and 67% of cholesterol) induces an ordering effect on SOPE *acyl* chains and provokes the formation of sterol-poor and sterol-rich domains which stoichiometry is independent of monolayer composition. The foregoing findings allow one to conclude that in cytosolic leaflet of membrane the lipids may segregate into domains of various cholesterol contents which depending on their composition may play different roles in membrane functioning.

1. Introduction

Phosphatidylethanolamines (PEs) are, after phosphatidylcholines (PCs), the most abundant phospholipids in mammalian membranes [1]. This group of glycerophospholipids displays wide biological functions, which are related for example to their metabolism in the heart and liver as well as their role as precursors in the synthesis of neurotransmitters (e.g. Anandamide) and glycosylphosphatidylinositol anchors for various proteins [2]. In cellular membranes of human erythrocytes PEs are localized mainly in the inner leaflet where they cover a significant mass of total phospholipids [3,4]. As the components of membrane PEs play a significant role in membrane fusion and they are important structural elements of bilayer [2,5]. Therefore, there are performed the investigations on the PE-containing artificial systems dedicated to explore the role of these phospholipids in estimation of the organization of various cellular membranes. The studies involve both the mixtures composed of PEs and other phospholipids imitating e.g. bacterial membranes [6] as well as PE/cholesterol model systems imitating the inner layer of e.g. mammalian membrane [7]. The latter systems are investigated mainly from the point of view of the effect of cholesterol on the organization and domain formation in cytosolic membrane layer. At this point it should be noted that the reports concerning the foregoing PE/cholesterol systems are much rarer as compared to those for mixtures composed of cholesterol and the outer layer lipids (phosphatidylcholine — PC, sphingomyelin — SM). On the other hand this is a very interesting task because the composition of both membrane leaflets is different and the major phospholipids in each membrane layers (PC — in the outer layer versus PE in the inner layer) differ significantly in their structure. The ability of ethanolamine moiety to interact via hydrogen bonds causes more favorable PE–PE interactions as compared to chol–PE forces and thus the mixing in PE/Chol system is limited [8] and the interactions of cholesterol in PE mixtures differ from those in PC-containing systems. This is directly connected with the structure of both phospholipids and undoubtedly may influence the organization of both membrane layers.

As it was widely evidenced the incorporation of cholesterol into PC or SM or PC/SM membranes induces the formation of liquid ordered (*lo*) phase [9] and it was postulated that *lo* domains in the outer layer are connected to those existing in the inner layer [10]. Although it is believed that domains are formed also in the inner layer, their nature and compositions are explored much less accurately as compared to the morphology of the outer layer [10–13]. As indicated the results presented in literature *lo* domains are formed in various cholesterol/PE mixtures [7,8,14,15]. It was also evidenced that the properties of these systems e.g. the interactions and miscibility of cholesterol with PEs in model systems, as well as the influence of cholesterol on the chain-melting phase transition temperature of the host PE bilayer and organization of membrane [7,16] are determined by various factors, e.g. the proportion of lipids in the mixture, structure of PE chains as

* Corresponding author. Tel.: +48 12 633 20 79; fax: +48 12 634 05 15.
E-mail address: wydro@chemia.uj.edu.pl (P. Wydro).

0005-2736/$ – see front matter © 2013 Elsevier B.V. All rights reserved.
http://dx.doi.org/10.1016/j.bbamem.2013.01.023

well as temperature. For example considering the solubility limit of cholesterol in PEs the X-ray diffraction experiments evidence the formation of crystalline cholesterol domains in mixtures with egg phosphatidylethanolamine (egg PE) or with dielaidoyl phosphatidylethanolamine (DEPE) at 35–40% of cholesterol, at 43% in DMPE [17] and at 51% in POPE-containing systems [18]. In general cholesterol was found to reflect better miscibility with PE possessing mono- and polyunsaturated chains as compared to the fully saturated [9].

From the point of view of membrane organization and considering inconsistencies in the results obtained for various Chol/PE systems postulated in literature [15] it is required to investigate the ability of cholesterol to form *lo* phase in PE environment and to analyze the properties of the formed domains. The investigations involving saturated PEs proved that they do not form complexes with cholesterol [19]. On the other hand recent investigations performed on monolayers and vesicles evidenced that 1-stearoyl-2-linoleoyl-sn-glycero-3-phosphatidyl-ethanolamine (SLPE) is able to form specific complexes with cholesterol, which may form nanoscale assemblies in the inner membrane layer. It was also suggested that other PE molecules containing unsaturated chains may form domains in the inner leaflet [14]. The aims of this work were to verify the formation of domains in cholesterol/SOPE films of various sterol contents and to characterize the properties of these domains and their composition. In these studies the Langmuir monolayer technique together with BAM was applied to investigate the miscibility and interactions between molecules in the mixtures as well as the domain formation in the studied films. To gain insight into the properties of the domains formed in the foregoing system GIXD experiments were performed.

2. Experimental

2.1. Materials

The investigated phospholipids, namely 1-stearoyl-2-oleoyl-*sn*-glycero-3-phosphoethanolamine (SOPE) as well as cholesterol (Chol) were synthetic products of high purity (≥99%) purchased from Avanti Polar Lipids, Inc. (700 Industrial Park Drive Alabaster, Alabama 35007-9105, USA). To prepare spreading solutions the lipids were dissolved in chloroform/methanol (4:1 v/v) mixture (both chloroform and methanol were purchased from Sigma-Aldrich, Poland, HPLC grade, ≥99.9%). From the respective stock solutions the mixed solutions were prepared and desirable volume of the latter was deposited onto the water subphase with the Hamilton micro syringe, precise to 1.0 μL. The volume of the spreading solutions was varied between 150 and 200 μL. Measurements were performed at 20 °C ± 0.1 °C and the temperature was controlled thermostatically by a circulating water system. Ultrapure Milli-Q water used as the subphase in the monolayer experiments at 20 °C ± 0.1 °C has surface tension of 72.6 mN/m and resistivity of 18.2 MΩ·cm.

2.2. Methods

Brewster angle microscopy experiments were performed with ultraBAM instrument (Accurion GmbH, Goettingen, Germany) equipped with a 50 mW laser emitting *p*-polarized light at a wavelength of 658 nm, a 10× magnification objective, polarizer, analyzer and a CCD camera. The spatial resolution of the BAM was 2 μm. The experiments were carried out with KSV 2000 Langmuir trough (KSV Instruments Ltd., Helsinki, Finland) (total area = 870 cm^2) equipped with two movable barriers. The microscope and the film balance were placed on a table (Standa Ltd, Vilnius, Lithuania) with active vibration isolation system (antivibration system VarioBasic_40, Halcyonics, Göttingen, Germany). The surface pressure was measured with the accuracy of ± 0.1 mN/m using a Wilhelmy plate made of filter paper (ashless Whatman Chr1) connected to an electrobalance. After spreading, the monolayers were left for solvent evaporation for 10 min and then the compression was initiated with the barrier speed of 5 cm^2/min (2.5 $Å^2 molec^{-1}\ min^{-1}$).

X-ray scattering experiments were performed at the BW1 (undulator) beamline at the HASYLAB synchrotron source (Hamburg, Germany) using a dedicated liquid surface diffractometer [20] with an incident X-ray wavelength λ ≈ 1.304 Å. A Teflon thermostatted Langmuir trough (Riegler & Kirstein, Potsdam, Germany), equipped with a movable barrier for monolayer compression, was placed in a gastight container and mounted on the diffractometer. After spreading the solution onto the subphase, at least 40 min was allowed for the trough container to be flushed with helium to reduce the scattering background and to minimize beam damage during X-ray scans. Then, the monolayers were compressed to the surface pressure of 32.5 mN/m (the surface pressure at which the properties of monolayer can be compared with those of bilayers in the natural membrane [21,22]), at which the X-ray experiments were performed. As far as the GIXD experiments are concerned, the X-ray scattering theory and the liquid diffractometer construction have been described previously [23–25].

3. Data analysis

To verify and compare the state of the investigated films and to obtain information on molecular ordering in monolayer from the isotherm data points the compression modulus values at a given monolayer composition were calculated according to Eq. (1) [26].

$$C_S^{-1} = -A\ (d\pi/dA)_T \tag{1}$$

where A is area per molecule at a surface pressure π. The ordering effect of cholesterol was analyzed by comparison of the variations of the compression modulus values with the addition of sterol at a given surface pressure.

The analysis of the condensing effect of cholesterol on phospholipid film was based on the values of the excess area per molecule in the mixed monolayer calculated as follows [27,28]:

$$A^{Exc} = A - A^{id} \tag{2}$$

wherein A is the mean area per lipid molecule in the mixed monolayer determined form isotherm at a given surface pressure whereas A^{id} denotes the molecular area resulting from the assumption of ideal mixing of the film components at the same π value.

The values of A^{id} for binary mixed monolayers were calculated on the basis of the equation:

$$A^{id} = X_1 A_1 + X_2 A_2 \tag{3}$$

A_1, A_2 are mean molecular areas of the respective lipids in their pure films at a given surface pressure and X_1, X_2 are the molar fractions of components 1 and 2 in the mixed film.

GIXD experiments provided the information on the lateral ordering of the samples. The scattered intensity was measured by scanning over a range of horizontal scattering vectors Q_{xy}:

$$Q_{xy} \approx \frac{4\pi}{\lambda} \sin\left(2\theta_{xy}/2\right) \tag{4}$$

where $2\theta_{xy}$ is the angle between the incident and diffracted beam projected on the liquid surface. The GIXD intensity resulting from a powder of 2D crystallites can be represented as Bragg peaks, resolved in the Q_{xy} direction, by integrating the scattered intensity over the Q_z direction, which is measured by the position-sensitive detector placed perpendicular to the air-water interface. Conversely,

the Bragg rod profiles were resolved in the Q_z direction and obtained by integrating the scattered intensity over Q_{xy} corresponding to the Bragg peak.

$$Q_z = \frac{2\pi}{\lambda} \sin\alpha_f \tag{5}$$

where α_f is the X-ray exit angle.

The in-plane lattice repeat distances d of the ordered structures in the monolayer were calculated from the Bragg peak positions:

$$d = \frac{2\pi}{Q_{xy}} \tag{6}$$

To evaluate the extent of crystalline order in the monolayer, the in-plane coherence length L_{xy} was approximated from the *fwhm* of the Bragg peaks using the Scherrer formula:

$$L_{xy} = 0.9\frac{2\pi}{fwhm_{Q_{xy}}} \tag{7}$$

where $fwhm_{Q_{xy}}$ is the full width at half maximum of the Bragg peak.

Similarly, from the *fwhm* of the Bragg rod, according to the Scherrer formula, the coherently scattering length of the molecule, (L_z) was calculated:

$$L_z = 0.9\frac{2\pi}{fwhm_{Q_z}} \tag{8}$$

Additionally, information about the molecular tilt angle (τ), which describes the deviation from the upright orientation of the film-forming molecules, was obtained from the equation:

$$Q_{z,hk} = Q_{xy} tg(\tau) \cos\psi \tag{9}$$

where ψ is the angle between tilt direction and the Q_{xy} vector.

The analysis procedure has been described in details elsewhere [29,30].

4. Results

Fig. 1A presents the surface pressure–area (π–A) isotherms recorded for one-component SOPE and Chol monolayers and their mixtures of various composition.

As can be noticed, in the case of SOPE monolayer the surface pressure starts to rise at the area of ca. 90 Å^2/molecule and it increases up to the area of ca. 40 Å^2/molecule, at which the monolayer collapses ($\pi_{coll.} \approx 56$ mN/m). Moreover, at the surface pressure of ca. 27 mN/m a plateau region, which corresponds to the minimum in the C_S^{-1} vs. surface pressure dependency (Fig. 1B), is seen. The maximal values of the compression modulus, divided by this minimum, indicate that during film compression its physical state changes from liquid to condensed. The addition of a small amount of cholesterol ($X_{Chol} = 0.1$) into SOPE film shifts the isotherm towards slightly larger areas and increases the surface pressure at which phase transition appears. Further addition of cholesterol provokes the shift of the isotherm to smaller areas and induces a decrease of the collapse surface pressure value. Moreover, it is visible that the increasing concentration of cholesterol in the mixed film causes the region of the phase transition to shorten and shift to the lower surface pressures. This tendency is easily observable in the compressional modulus (C_S^{-1}) versus the surface pressure curves (Fig. 1B), where pseudo-plateau appears as a minimum. Both the changes in the position of plateau region as well as the variations in the collapse surface pressure may indicate miscibility of the monolayer's components.

To verify the effect of cholesterol on the packing of molecules in the mixed film and confirm the miscibility between molecules the mean

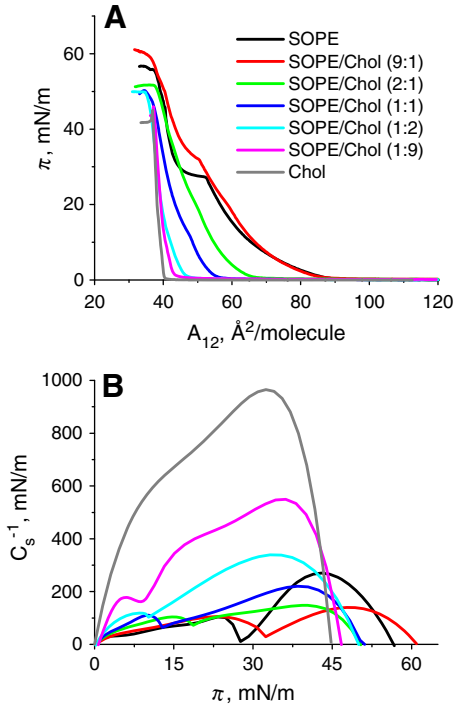

Fig. 1. The surface pressure–area isotherms (A) and compression modulus (C_s^{-1}) values vs. the surface pressure plots (B) for the investigated monolayers.

area per molecule (A_{12}) values were estimated from the isotherms at three different values of the surface pressure (5, 15, and 32.5 mN/m) and compared with those resulting from additivity rule (A^{id}).

As it is seen (Fig. 2) the mean molecular areas deviate from additivity indicating a non-ideal behavior of the mixed monolayers. Moreover, at low concentration of cholesterol the values A_{12} are larger than those resulting from the additivity rule whereas at higher cholesterol content the situation is opposite indicating film condensation. To analyze the magnitude of condensation induced by the addition of cholesterol into SOPE film, the excess area per molecule values were calculated and presented in a function of sterol concentration in Fig. 3.

Analyzing Fig. 3 one can see that the system behaves non-ideally which results from different interactions between molecules in the mixed monolayers as compared to those in one-component films. Moreover, it is worth to notice that at low surface pressure the values of A^{Exc} are lower as compared to those at higher π. This is due to more fluid (chain-disordered) character of pure SOPE monolayer (at lower π)

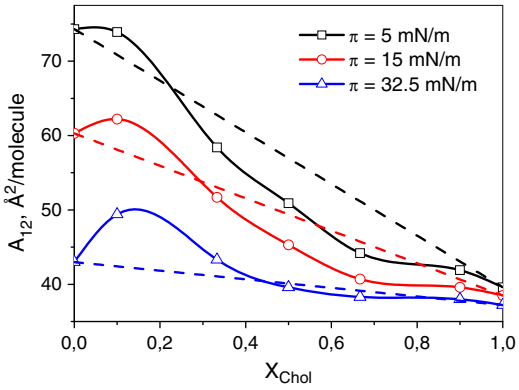

Fig. 2. The mean molecular area vs. cholesterol molar fraction plots for the investigated monolayers.

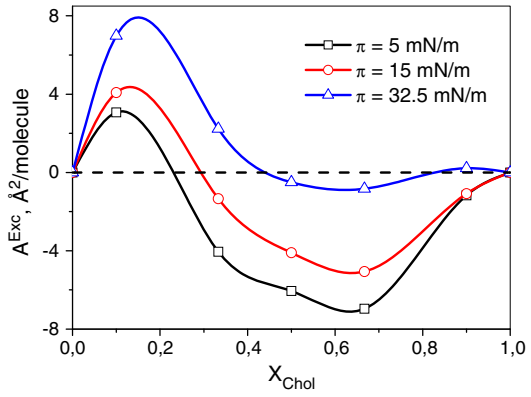

Fig. 3. The excess molecular area vs. cholesterol molar fraction plots for the investigated monolayers.

which in this state is more susceptible to the area contraction provoked by cholesterol. At higher surface pressures the SOPE film is much more condensed and therefore it is less prone to area condensation but more sensitive to its expansion, which reflects more positive values of A^{Exc} at low cholesterol content and less negative excess areas at higher sterol concentrations.

To evaluate the effect of cholesterol on the elasticity of SOPE film the values of the compressional modulus (C_S^{-1}) at $\pi = 32.5$ mN/m were plotted as a function of the monolayer's composition (Fig. 4).

As it can be observed in Fig. 4 the compressional modulus values increase with the content of cholesterol in the mixed film, except for the mixture containing only 10% of sterol. In this case a decrease of this parameter suggests a disordering effect of cholesterol on SOPE film. Further addition of sterol induces systematic ordering of phospholipid monolayer.

The investigated mixed films were visualized by using Brewster angle microscope. BAM images taken at various stages of the films' compression are presented in Fig. 5.

Analyzing BAM images for pure SOPE monolayer, at large areas a coexistence of gaseous (dark regions) and liquid phase can be observed. During film compression the gaseous phase vanishes and the monolayer becomes homogenous up to the pressure where small light domains of more condensed phase appear. Further decrease of the mean molecular area causes these domains' growth. Above the region of phase transition, which manifests as a plateau in the isotherm, condensed domains merge together and form homogenous film. However, at higher surface pressure small light spots of a new phase can be seen. The existence of similar domains, which probably represent the solid phase, was also found by other authors in very similar POPE monolayer [31,32]. As regards cholesterol its

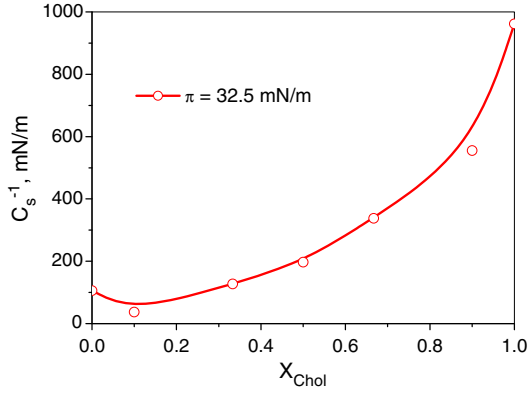

Fig. 4. The variation of the compression modulus values (C_s^{-1}) with the composition of monolayer at $\pi = 32.5$ mN/m.

monolayer is completely homogenous in a very wide range of surface pressures except for the regions of large areas per molecule and $\pi = 0$ mN/m where condensed domains dispersed in gaseous phase can be observed. The addition of small amount of cholesterol ($X_{Chol} = 0.1$) into SOPE film causes the condensed structures to form at slightly higher surface pressure which are much smaller as compared to those formed in pure phospholipid's film. Further increase of cholesterol concentration causes the condensed domains to start to appear at lower surface pressures, which corroborates with the drop of π at which the plateau region appeared in the isotherms. These are the only differences in the pictures taken for monolayers containing 33, 50 and 67% of cholesterol, therefore in Fig. 5 only the images for one of the foregoing system are shown. With the films' compression the number of these domains increases, however, contrary to the pure SOPE film, these structures are very small and their size does not change up to the monolayer's collapse. In the case of mixtures containing 90 mol% of cholesterol the morphology of the film is practically the same as for pure monolayer of sterol (data not shown).

To study the in-plane organization of the investigated monolayers the GIXD method was applied. The GIXD data collected for pure films of the investigated lipids, at the surface pressure $\pi = 32.5$ mN/m, are presented in Figs. 6 and 7.

For pure film of cholesterol the diffracted intensity plotted as a function of the in-plane scattering vector component (Q_{xy}) shows one diffraction signal (Fig. 6A). The corresponding Bragg rod presented in Fig. 6B indicates that the maximum intensity of the Bragg peak is localized at the horizon, i.e., at $Q_z = 0$ Å^{-1}. This indicates that in the monolayer, at the investigated surface pressure, molecules are closely packed in 2D hexagonal lattice with the hydrophobic part oriented perpendicularly to the air/water interface.

In contrast to the cholesterol film, the analysis of the in-plane diffraction scans for different Q_z intervals as well as Bragg rods, for the SOPE monolayer, clearly indicates that two diffraction peaks (Fig. 7A) and two rods (Fig. 7B) can be distinguished. Moreover, it is seen that the position of the most intense peak has its maximum at the horizon ($Q_z = 0$), while the second Bragg peak denoted as (−1, 1) is localized at $Q_{xy} = 1.47$ Å^{-1} with its maximum at $Q_z = 0.19$ Å^{-1}. Such an intensity distribution is characteristic for the monolayer in which molecules are organized in the centered rectangular lattice with the molecular tilt turned toward the nearest neighbor (NN) [33].

In the case of the mixtures containing 10 mol% of cholesterol, similarly to the SOPE film, two diffraction peaks (Fig. 8) and two Bragg rods (data not shown), indicating centered rectangular lattice with tilted hydrophobic parts of molecules, can be distinguished. However, the positions of these peaks lead to slightly larger lattice constants and larger tilt of the hydrophobic parts as compared to pure SOPE film (Table 1). Moreover, broadening of the Bragg peaks suggests that the extent of the in-plane order is smaller as compared to the one-component phospholipid film.

With the further addition of cholesterol (i.e. 33.3, 50 and 66.7 mol%) only one diffraction peak localized at Q_{xy} ca. 1.5 can be found. Moreover, with cholesterol addition the intensity of this peak significantly decreases, however its position does not change (Fig. 9). For better comparison the plots of diffracted intensity vs. Q_{xy} for these mixtures were presented in one figure (Fig. 9).

It is worth to see that, in the 2D diffractograms registered for the foregoing films, besides the peak localized at $Q_{xy} \approx 1.5$ an additional diffraction signal situated at $Q_{xy} \approx 1.2$ can be observed. Also in this case the position of the peak does not change with the increase of sterol concentration, however, its intensity increases. The analysis of the Bragg rods (data not shown) indicates that for both peaks the maximum intensity is localized at $Q_z = 0$, which means that in both types of crystalline domains the molecules are packed hexagonally with the hydrophobic part oriented perpendicularly to the air/water interface.

As regards the monolayer containing 90 mol% of cholesterol only one Bragg peak (Fig. 10) as well as one Bragg rod (data not shown)

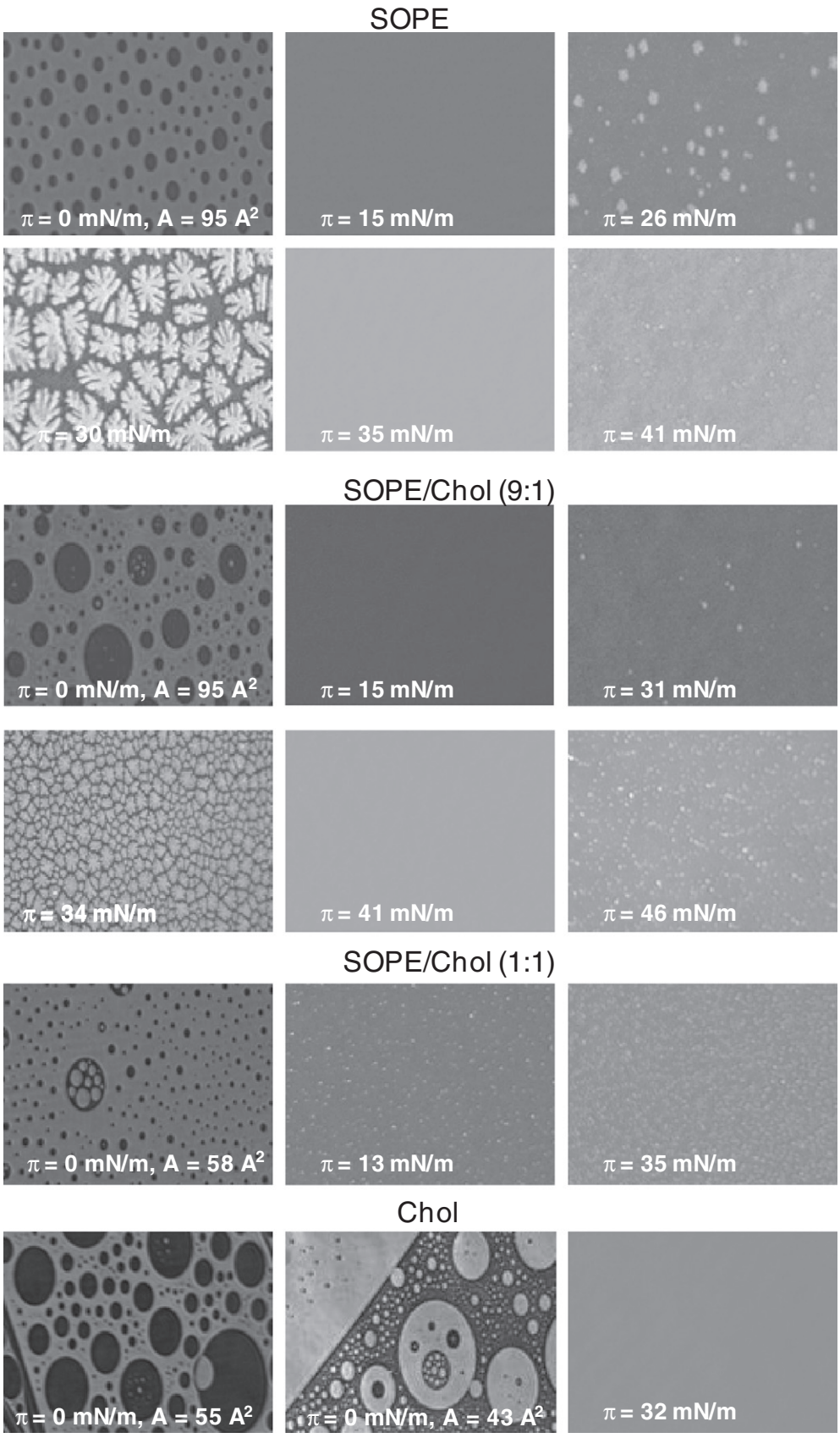

Fig. 5. BAM images taken for the investigated monolayers at different stages of compression.

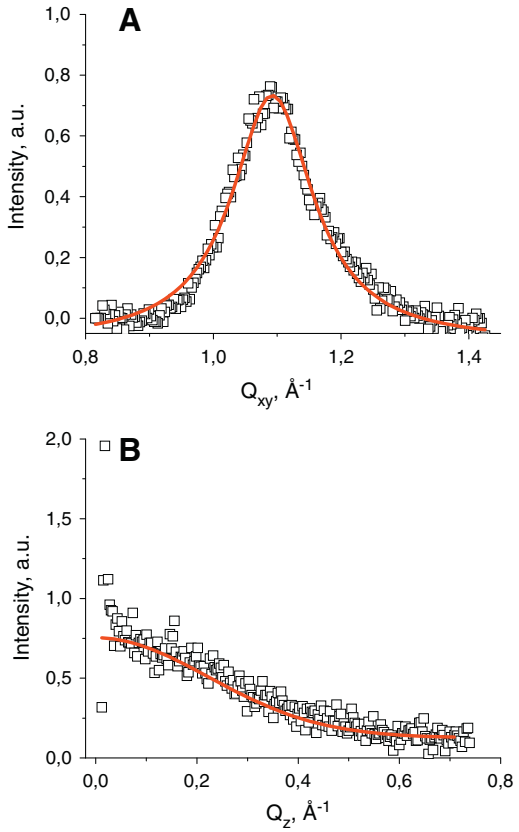

Fig. 6. Background-subtracted GIXD diffraction data (points) and fit (solid lines) for cholesterol monolayers compressed to 32.5 mN/m. (A) Bragg peak profile *I*(*Qxy*) and corresponding Bragg rod profile *I*(*Qz*).

can be found. Moreover, the position of the diffraction peak is practically the same as for pure cholesterol film indicating significant similarity between those monolayers.

5. Discussion

In membranes of human erythrocytes phosphatidylcholines are presented mainly in the outer layer, while ca. 80% of total membrane phosphatidylethanolamines accumulate in the inner leaflet of bilayer [34]. Both these phospholipids classes comprise significant mass of the lipids in the respective membrane leaflets and therefore strongly determine layers properties. Although PC and PE differ markedly in the structure and properties of polar head as well as in the behavior in membrane environment, the investigations concerning the organization of phosphatidylethanolamine-containing model systems are performed much rarely as compared to those performed for the PC species. This fact has stimulated the investigations done in this paper aimed at a comprehensive analysis of molecular organization of SOPE/cholesterol mixtures of various composition.

As regards one-component SOPE film, it was found that monolayer undergoes a phase transition from liquid to condensed state. Thus the properties of the SOPE monolayer are significantly different from those published for its phosphatidylcholine counterpart namely stearoyl-oleoyl phosphatidylcholine (SOPC) [35] that even at higher surface pressures forms typically liquid film. Since both phospholipids contain the same hydrophobic group the foregoing differences are determined by the structure of their polar moieties. First of all, the choline group of SOPC is larger than the ethanolamine group of SOPE. Moreover, in contrast to phosphatidylcholines, phosphatidylethanolamines are able to form intermolecular hydrogen bonds between the ammonium and the phosphate group of the neighboring molecules. All of these cause the PE molecules to pack denser than the PCs, which strongly reduces the fluidizing effect of *cis* double bond within *sn*-2 chain in SOPE molecule. A very close packing of SOPE molecules additionally forces the ordering of their hydrophobic chains manifested in the obtained diffractogram. The GIXD data clearly show that, at the biologically

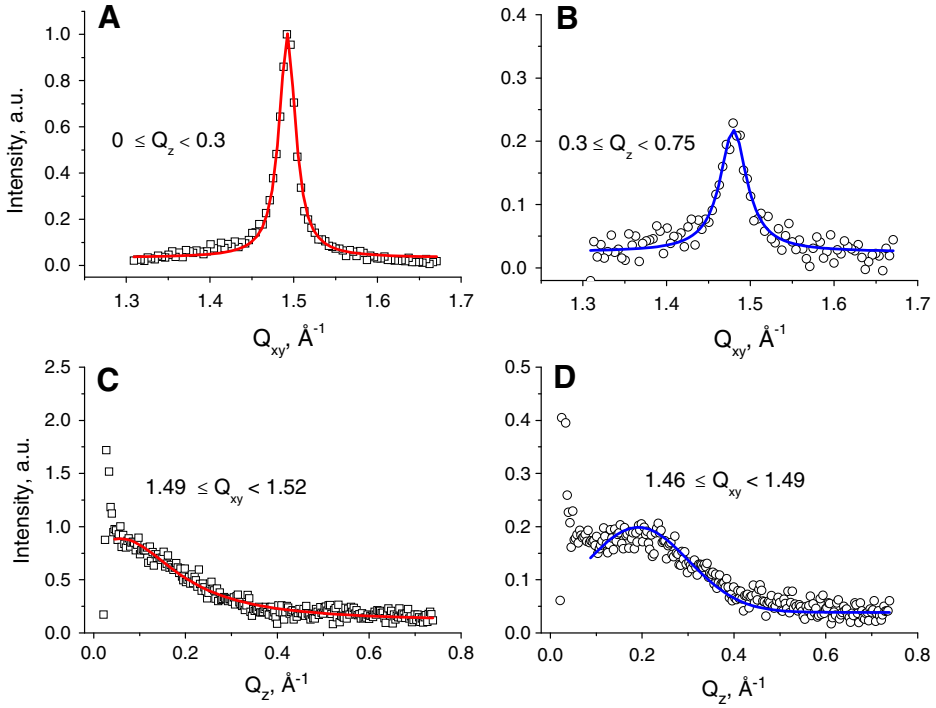

Fig. 7. Background-subtracted GIXD diffraction data (points) and fit (solid lines) for SOPE monolayer compressed to 32.5 mN/ m. (A,B) Bragg peak profiles *I*(*Qxy*) integrated over the Q_{xy} regions indicated on the graph. The Bragg peaks were fitted using Lorentzian function. (C, D) Corresponding Bragg rod profiles *I*(*Qz*). The Bragg rods were integrated over the Q_{xy} regions indicated on the graph. The distribution of the scattered intensity along the Bragg rods was fitted using Gaussian function.

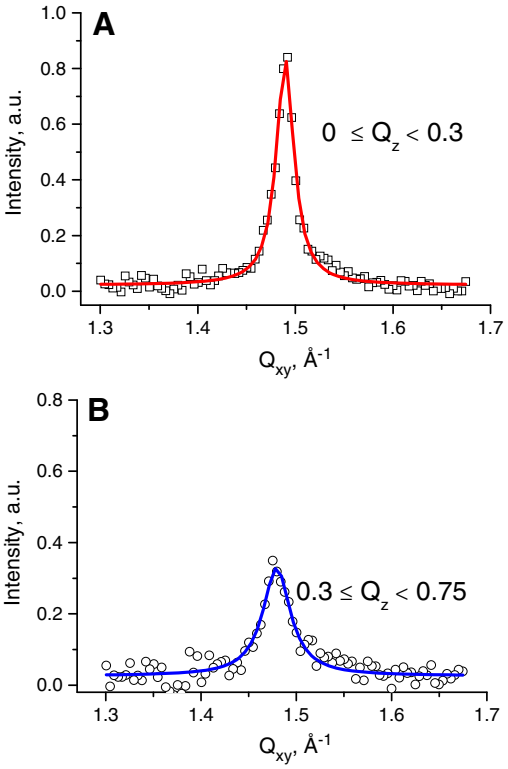

Fig. 8. Background-subtracted GIXD diffraction data (points) and fit (solid lines) for SOPE/Chol (9:1) monolayer compressed to 32.5 mN/m. (A,B) Bragg peak profiles $I(Qxy)$ integrated over the Q_{xy} regions indicated on the graph. The Bragg peaks were fitted using Lorentzian function.

relevant surface pressure, in the SOPE monolayer crystalline domains are formed. In these structures the molecules are organized into centered rectangular lattice with hydrophobic chains tilted towards the nearest neighbor (NN). The tilt of the chains in the SOPE monolayer was found to be of 8.5° and it is much smaller as compared to that for DPPC (29° [36]), containing two fully saturated chains in the molecule. These differences are due to the interactions between PEs via hydrogen bonds and smaller cross-section area of the PE than the PC group.

Strong intermolecular attractions between the PE groups manifest also in the results obtained for the SOPE/Chol mixtures. It was found that all the investigated mixtures show deviations from ideal miscibility, which indicates that the interactions between molecules in the mixed films differ from those in the respective one-component monolayers. It was found that the addition of small amount of

Table 1
In-plane structural parameters obtained from GIXD experiments for SOPE, Chol and their mixed monolayers at the surface pressure $\pi = 32.5$ mN/m: a and b — the lengths of the unit cell vectors, γ — the angle between the vectors a and b, τ — tilt angle, L_{xy} — in-plane coherence length, L_z — the length of the coherently scattering molecular moiety, A_{uc} — area of the 2D unit cell, A — mean molecular area.

Composition of monolayer	Q_{xy} (Å^{-1})	Q_z (Å^{-1})	a, b (Å)	γ (°)	τ (°)	L_{xy} (Å)	L_z (Å)	A_{uc} (Å^2)
SOPE	1.492	0	4.920	90	8.5	246	21	41.44
	1.479	0.19	8.422			160		
SOPE/Chol (9:1)	1.488	0	4.934	90	8.9	230	17.7	41.67
	1.475	0.20	8.445			145		
SOPE/Chol (2:1)	1.493	0	4.859	120	0	188	16.1	20.45
	1.198	0	6.056	120	0	52	11.5	31.76
SOPE/Chol (1:1)	1.494	0	4.856	120	0	191	15.8	20.42
	1.196	0	6.066	120	0	48	11.1	31.87
SOPE/Chol (1:2)	1.494	0	4.856	120	0	187	15.9	20.42
	1.197	0	6.061	120	0	47	11.3	31.81
SOPE/Chol (1:9)	1.103	0	6.578	120	0	30	12.3	37.47
Chol	1.094	0	6.628	120	0	36	12.7	38.04

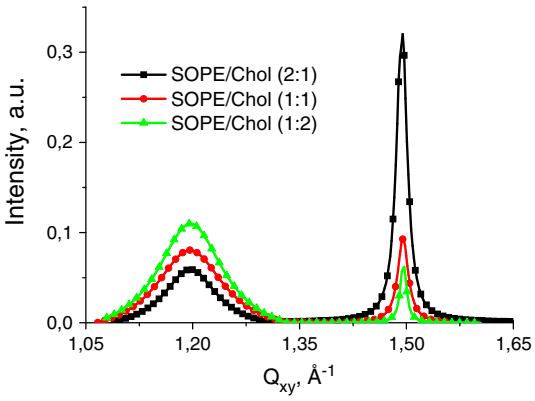

Fig. 9. Bragg peak $I(Qxy)$ profiles for SOPE/Chol monolayers of various composition compressed to the surface pressure of 32.5 mN/m.

cholesterol into the SOPE film causes its expansion whereas for higher concentrations of sterol the contraction of the area can be observed. Moreover, the obtained results point out that also the chain-ordering is dependent on the sterol concentration and for the mixed film containing 10 mol% of cholesterol it is lower as compared to the pure SOPE monolayer and increases with further sterol addition The foregoing results were additionally confirmed by the BAM images and GIXD measurements, which provide very useful information on the molecular organization of the crystalline domains in thin films in the angstrom scale. The GIXD results obtained for the mixed film at 10% of cholesterol prove that in the crystalline domains the molecules are organized into centered rectangular lattice, which is similar to the organization of molecules in the pure SOPE film. However, the tilt of hydrophobic chains was found to be slightly larger as compared to that in the one-component SOPE film. For this mixture also the L_{xy}, values indicating in-plane coherence length are smaller than for the SOPE monolayer. These results allow one to conclude that the incorporation of small amount of cholesterol into the SOPE film disorders a condensed structure of pure phospholipids film. This is a consequence of a weakening of the interactions via hydrogen bonds between SOPE molecules caused by the presence of sterol molecules. This effect manifests in the expansion of the mixed film resulting in a larger mean area per molecule values for SOPE/Chol mixture as compared to SOPE film as well as in a lower ordering of the former monolayer.

The properties of the SOPE/cholesterol film change with the increase of sterol content in the system and as it was mentioned earlier further addition of cholesterol induces condensation of the film and increases its ordering. The analysis of GIXD data evidences the existence of two

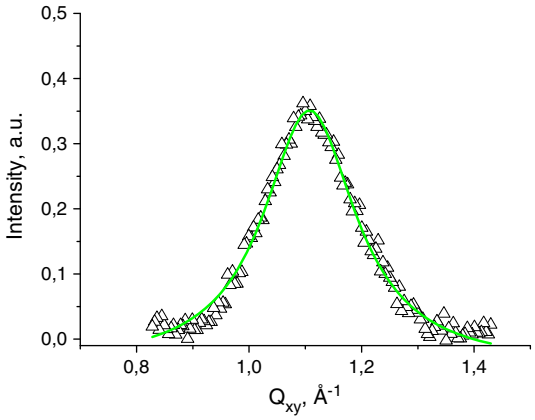

Fig. 10. Bragg peak $I(Qxy)$ profile for SOPE/Chol (1:9) monolayers compressed to the surface pressure of 32.5 mN/m.

Bragg peaks for each monolayer localized at Q_{xy} similar to that for the one-component films of cholesterol and SOPE, respectively. It was also found that the intensity of the Bragg peaks for the mixed films changes with the content of sterol in the mixed monolayer, however, their position is always the same. The analysis of the diffraction data proves hexagonal packing of molecules in the crystalline domains and the orientation of their hydrophobic part perpendicularly to the air/water interface. Moreover, one can see that the values of L_z which are connected with the length of the scattering part of the molecules differ from those determined for the respective pure monolayers (Table 1) which clearly evidences that the domains consist of both components of the mixed film. Therefore, it can be concluded that the presence of two Bragg peaks in diffractograms for the mixed films corresponds to the existence of two different kinds of crystalline domains of fixed stoichiometry. Moreover, their positions which are independent of monolayer composition indicate that one type of these domains is enriched in SOPE whereas the second is richer in cholesterol. This is also proved by the opposite change of the intensity of the peaks at lower and higher values of Q_{xy} with the increase of cholesterol content in the mixed film. Furthermore, the broadening of the diffraction peaks resulting in lower values of L_{xy} (Table 1) designates that the crystalline structures in the mixed film are smaller than those in pure phospholipid film which is consistent with the observation that cholesterol perturbs the gel phase in phospholipids bilayers forming L_o phase [37].

In contrast to the foregoing mixtures for the monolayers containing 90% of cholesterol one can see only one Bragg peak located at nearly the same value of Q_{xy} as for pure cholesterol film. However, the intensity of this peak is lower and it is somewhat broaden with respect to that obtained for the one-component sterol monolayer. This indicates that for this mixture the ordered domains consisting practically of pure cholesterol are formed from smaller fraction of monolayer material and are smaller than those in the one-component sterol film.

7. Conclusions

The surface pressure–area measurements, the analysis of BAM images as well as GIXD data collected in this work for SOPE/cholesterol mixed monolayers of various composition provided an extensive information on the properties of these systems, which may be important from the point of view of the organization of cytosolic leaflet of mammalian membrane. It was evidenced that SOPE and cholesterol mix non-ideally in the wide range of the films composition. At lower content of sterol in the system (10%) its disturbing influence on SOPE film was proved, however further addition of sterol was found to induce the ordering of monolayers. Moreover, at 33, 50 and 67% of sterol in the mixed film the formation of two kinds of domains in the system was proved. As far as their composition is concerned one of them is richer in cholesterol, while the other in SOPE. Interestingly the composition of these domains is independent on the content of cholesterol in the monolayer. This behavior is different from that reported previously for DPPC/Chol monolayers [38] for which the composition of the formed domains reflected that the composition of the film is changed with cholesterol concentration.

The observed phase separation into cholesterol-rich and sterol-poor domains in the investigated SOPE/Chol films may result from the adverse interactions between phosphatidylethanolamines and cholesterol which is suggested also by other authors [39–41]. Moreover, the fact that phosphatidylethanolamines provide unfavorable environment for cholesterol may lead to partial externalization of cholesterol molecules from the inner to outer membrane leaflet [41,42] dominated by the lipids (phosphathidylcholines and sphingomyelines) interacting beneficially with sterols. Thus taking into account that majority of cholesterol may be located in the outer monolayer of erythrocyte membrane the SOPE/cholesterol mixtures of lower cholesterol level (up to 33% of cholesterol) seem to be the most proper as the model of the inner leaflet of membrane. However, as it was found even at lower concentration cholesterol strongly disturbs the SOPE film leading to the formation of highly ordered domains.

Additionally, the obtained results give some insight into the issue of raft formation in cytosolic leaflet of membrane. Namely, they may suggest that in the inner layer of the membrane dominated by PE species and containing cholesterol the domains enriched in cholesterol and SOPE may exist. This is a highly important finding taking into account that the composition and properties of the rafts in the inner layer are much less explored as compared to those formed in the outer layer [10,12]. Moreover, as it was found [42] some transmembrane proteins incorporate into cholesterol-rich domains or for their proper functioning cholesterol is required. Therefore it can be hypothesized that sterol-rich domains may be clustering by proteins (e.g. annexins, flotillins or other scaffolding being clustering agents in raft in inner layer [11]) and specialized in participating in various vitally important membranes' processes, e.g. signal transduction.

Acknowledgement

The Authors are grateful to DESY-HASYLAB, Hamburg (Germany) for granting synchrotron beam time for the realization of the project.

The research was carried out with the equipment (ultraBAM) purchased thanks to the financial support of the European Regional Development Fund in the framework of the Polish Innovation Economy Operational Program (Contract No. POIG.02.01.00-12-023/08).

References

[1] E. Sackmann, Biological membranes architecture and function, in: R. Lipowski, E. Sackmann (Eds.), Structure and Dynamics of Membranes, Elsevier, Amsterdam, 1995, pp. 1–64.
[2] J.E. Vance, Phosphatidylserine and phosphatidylethanolamine in mammalian cells: two metabolically related aminophospholipids, J. Lipid Res. 49 (2008) 1377–1387.
[3] J.A. Virtanen, K.H. Cheng, P. Somerharju, Phospholipid composition of the mammalian red cell membrane can be rationalized by a superlattice model, Proc. Natl. Acad. Sci. U. S. A. 95 (1998) 4964–4969.
[4] G. Karp, Cell and Molecular Biology: Concepts and Experiments, fourth ed. Wiley & Sons, New York, 2004. , (Chapter 4).
[5] P.M. Kasson, V.S. Pande, Control of membrane fusion mechanism by lipid composition: predictions from ensemble molecular dynamics, PLoS Comput. Biol. 3 (2007) 2228–2238.
[6] L. Picas, C. Suárez-Germà, M.T. Montero, Ó. Doménech, J. Hernández-Borrell, Miscibility behavior and nanostructure of monolayers of the main phospholipids of *Escherichia coli* inner membrane, Langmuir 28 (2012) 701–706.
[7] T.P.W. McMullen, R.N.A.H. Lewis, R.N. McElhaney, Calorimetric and spectroscopic studies of the e¡ects of cholesterol on the thermotropic phase behavior and organization of a homologous series of linear saturated phosphatidylethanolamine bilayers, Biochim. Biophys. Acta 1416 (1999) 119–134.
[8] A.G. Sostarecz, C.M. McQuaw, A.G. Ewing, N. Winograd, Phosphatidylethanolamine induced cholesterol domains chemically identified with mass spectrometric imaging, J. Am. Chem. Soc. 126 (2004) 13882–13883.
[9] H. Ohvo-Rekilä, B. Ramstedt, P. Leppimäki, J.P. Slotte, Cholesterol interactions with phospholipids in membranes, Prog. Lipid Res. 41 (2002) 66–97.
[10] K. Simons, W.L.C. Vaz, Model systems, lipid rafts, and cell membranes, Annu. Rev. Biophys. Biomol. Struct. 33 (2004) 269–295.
[11] K. Simons, R. Ehehalt, Cholesterol, lipid rafts, and disease, J. Clin. Invest. 110 (2002) 597–603.
[12] P.A. Janmey, P.K.J. Kinnunen, Biophysical properties of lipids and dynamic membranes, Trends Cell Biol. 16 (2006) 538–546.
[13] P.F. Devaux, R. Morris, Transmembrane asymmetry and lateral domains in biological membranes, Traffic 5 (2004) 241–246.
[14] M. Grzybek, J. Kubiak, A. Łach, M. Przybyło, A.F. Sikorski, A raft-associated species of phosphatidylethanolamine interacts with cholesterol comparably to sphingomyelin. A Langmuir–Blodgett monolayer study, PLoS One 4 (2009) e5053.
[15] D.A. Mannock, R.N.A.H. Lewis, T.P.W. McMullen, R.N. McElhaney, The effect of variations in phospholipid and sterol structure on the nature of lipid–sterol interactions in lipid bilayer model membranes, Chem. Phys. Lipids 163 (2010) 403–448.
[16] C. Paré, M. Lafleur, Polymorphism of POPE/cholesterol system: a ^{2}H nuclear magnetic resonance and infrared spectroscopic investigation, Biophys. J. 74 (1998) 899–909.
[17] D. Bach, E. Wachtel, Phospholipid/cholesterol model membranes: formation of cholesterol crystallites, Biochim. Biophys. Acta 1610 (2003) 187–197.
[18] J. Huang, G.W. Feigenson, A microscopic interaction model of maximum solubility of cholesterol in lipid bilayers, Biophys. J. 76 (1999) 2142–2157.

[19] X. Wang, P.J. Quinn, Cubic phase is induced by cholesterol in the dispersion of 1-palmitoyl-2-oleoyl-phosphatidylethanolamine, Biochim. Biophys. Acta 1564 (2002) 66–72.
[20] J. Majewski, R. Popovitz-Biro, W.G. Bouwman, K. Kjaer, J. Als-Nielsen, M. Lahav, L. Leizerowitz, The structural properties of uncompressed crystalline monolayers of alcohols C_nH_{2n+1} OH ($n=13$–31) on water and their role as ice nucleators, Chem. Eur. J. 1 (1995) 304–311.
[21] H. Brockman, Lipid monolayers: why use half a membrane to characterize protein–membrane interactions? Curr. Opin. Struct. Biol. 9 (1999) 438–443.
[22] D. Marsh, Lateral pressure in membranes, Biochim. Biophys. Acta 1286 (1996) 183–223.
[23] T.R. Jensen, K. Kjaer, in: D. Mobius, R. Miller (Eds.), Novel Methods to Study Interfacial Monolayers, Elsevier, Amsterdam, The Netherlands, 2001, p. 205, (27–29).
[24] J. Als-Nielsen, K. Kjaer, in: T. Riste, D. Sherrington (Eds.), Proceedings of the NATO Advanced Study Institute, Phase Transitions in Soft Condensed Matter, Plenum Press, New York, 1989, p. 113.
[25] J. Als-Nielsen, D. Jacquemain, K. Kjaer, F. Leveiller, M. Lahav, L. Leiserowitz, Principles and applications of grazing incidence X-ray and neutron scattering from ordered molecular monolayers at the air–water interface, Phys. Rep. 246 (1994) 251–313.
[26] J.T. Davies, E.K. Rideal, Interfacial Phenomena, Academic Press, New York, 1963.
[27] I.S. Costin, G.T. Barnes, Two-component monolayers II. Surface pressure–area relations for the octadecanol-docosyl sulphate system, J. Colloid Interface Sci. 51 (1975) 106–121.
[28] G.L. Gaines Jr., Insoluble Monolayers at Liquid–Gas Interfaces, Interscience, New York, 1966.
[29] J. Als-Nielsen, H. Möhwald, Handbook on Synchrotron Radiation, in: S. Ebashi, M. Koch, E. Rubinstein (Eds.), Elsevier, North-Holland, Amsterdam, 1991, p. 1.
[30] M. Tanaka, M.F. Schneider, G. Brezesinski, In-plane structures of synthetic oligolactose lipid monolayers—impact of saccharide chain length, Chem. Phys. Chem. 4 (2003) 1316–1322.
[31] Ó. Domènech, J. Ignés-Mullol, M.T. Montero, J. Hernandez-Borrell, Unveiling a complex phase transition in monolayers of a phospholipid from the annular region of transmembrane proteins, J. Phys. Chem. B 111 (2007) 10946–10951.
[32] K. Hąc-Wydro, R. Lenartowicz, P. Dynarowicz-Łątka, The influence of plant stanol (β-sitostanol) on inner leaflet of human erythrocytes membrane modeled with the Langmuir monolayer technique, Colloids Surf. B 102 (2013) 178–188.
[33] V.M. Kaganer, H. Möhwald, P. Dutta, Structure and phase transitions in Langmuir monolayers P, Rev. Mod. Phys. 71 (1999) 779–819.
[34] Y. Yawata, Cell membrane: the red blood cell as a model, Wiley–VCH Verlag GmbH & Co. KGaA, Weinheim, 2003.
[35] P. Wydro, S. Knapczyk, M. Łapczyńska, Variations in the condensing effect of cholesterol on saturated versus unsaturated phosphatidylcholines at low and high sterol concentration, Langmuir 27 (2011) 5433–5444.
[36] K. Hąc-Wydro, M. Flasiński, M. Broniatowski, P. Dynarowicz-Łątka, J. Majewski, Properties of β-sitostanol/DPPC monolayers studied with grazing incidence X-ray diffraction (GIXD) and Brewster angle microscopy, J. Colloid Interface Sci. 364 (2011) 133–139.
[37] G.W. Feigenson, Phase diagrams and lipid domains in multicomponent lipid bilayer mixtures, Biochim. Biophys. Acta 1788 (2009) 47–52.
[38] A. Ivankin, I. Kuzmenko, D. Gidalevitz, Cholesterol–phospholipid interactions: new insights from surface X-ray scattering data, Phys. Rev. Lett. 104 (2010) 108101.
[39] Y. Lange, Tracking cell cholesterol with cholesterol oxidase, J. Lipid Res. 33 (1992) 315–321.
[40] K. House, D. Badgett, A. Abert, Cholesterol movement between bovine rod outer segment disk membranes and phospholipid bilayers, Exp. Eye Res. 49 (1989) 561–572.
[41] R. Pankov, T. Markovska, R. Hazarosova, P. Antonov, L. Ivanova, A. Momchilova, Cholesterol distribution in plasma membranes of β1 integrin-expressing and β1 integrin-deficient fibroblasts, Arch. Biochem. Biophys. 442 (2005) 160–168.
[42] K. Boesze-Battaglia, S.T. Clayton, R.J. Schimmel, Cholesterol redistribution within human platelet plasma membrane: evidence for a stimulus-dependent event, Biochemistry 35 (1996) 6664–6673.